


 CrossMark
click for updates

 Cite this: *Lab Chip*, 2014, 14, 3690

 Received 23rd April 2014,
Accepted 23rd July 2014

DOI: 10.1039/c4lc00479e

www.rsc.org/loc

Rapid and high-throughput formation of 3D embryoid bodies in hydrogels using the dielectrophoresis technique†

 Samad Ahadian,^a Shukuyo Yamada,^b Javier Ramón-Azcón,^{*acd} Kosuke Ino,^b Hitoshi Shiku,^b Ali Khademhosseini^{aefghi} and Tomokazu Matsue^{ab}

In this manuscript, we demonstrate the rapid formation of three-dimensional (3D) embryonic stem cell (ESC) aggregates with controllable sizes and shapes in hydrogels using dielectrophoresis (DEP). The ESCs encapsulated within a methacrylated gelatin (GelMA) prepolymer were introduced into a DEP device and, upon applying an electric field and crosslinking of the GelMA hydrogel, formed 3D ESC aggregates. Embryoid bodies (EBs) fabricated using this method showed high cellular viability and pluripotency. The proposed technique enables production of EBs on a large scale and in a high-throughput manner for potential cell therapy and tissue regeneration applications.

Embryonic stem cells (ESCs) are pluripotent cells that can renew themselves and differentiate into one or more specialized cell types having specific functions in the body.¹ Formation of embryoid bodies (EBs) is an early stage in the differentiation process of ESCs. EBs are three-dimensional (3D) aggregates of packed stem cells which have many

characteristics of early-stage embryos.² Three commonly used methods for forming EBs are liquid suspension culture of stem cells in dishes,³ stem cell culture in methylcellulose semisolid media,⁴ and the hanging drop method.⁵ Other methods include the use of microwell plates,⁶ spinner flasks,⁷ and stirred bioreactors⁸ for the production of large numbers of EBs. A major disadvantage of these methods is that they rely on the natural aggregation of stem cells and often provide poor control over EB size and distribution.

Microscale technologies have emerged as potentially useful tools in tissue engineering and biological applications.^{9–11} Such technologies render precise positioning of cells to define cell–cell and cell–extracellular matrix (ECM) interactions, mimicking the structure of native biological structures. Dielectrophoresis (DEP) is one of the various microscale technologies used in tissue engineering and cell manipulation studies.¹² The DEP approach can also be used for the rapid manipulation of other particles in the medium. For example, microparticles have been aggregated, separated, and trapped using DEP.^{13–16} Using this technique, particles are manipulated based on their interactions with an AC electric field, leading to charge polarization in the particles and their surrounding medium. When an underlying particle is more polarizable than its surrounding medium, the DEP force directs the particle towards high electric field regions. This phenomenon denotes positive DEP (p-DEP). Negative DEP (n-DEP) occurs when a particle is less polarizable than its suspending medium in the presence of a non-uniform electric field and is characterized by the escape of the particle from high electric field regions. Mammalian cells can be exposed to p-DEP forces without any adverse impact. For instance, Lu *et al.* showed that p-DEP had no adverse effect on the viability, proliferation, and differentiation of neural stem cells.¹⁷ An immobilization step is required after application of DEP forces to keep the dielectrophoretically manipulated cells in place. Recently, we proposed a promising approach to restrain dielectrophoretically patterned cells by encapsulating them within a methacrylated gelatin (GelMA)

^a WPI-Advanced Institute for Materials Research, Tohoku University, 2-1-1 Katahira, Aoba-ku, Sendai 980-8577, Japan. E-mail: ramonazconjavier@gmail.com; Fax: +81 22 217 6140; Tel: +81 22 217 6140

^b Graduate School of Environmental Studies, Tohoku University, Sendai 980-8579, Japan

^c Department of Chemical and Biomolecular Nanotechnology, Advanced Chemical Research Institute of Catalonia (IQAC-CSIC), Jordi Girona 18-26, Barcelona 08034, Spain

^d Nanobiotechnology for Diagnostics (Nb4D) Group, IQAC-CSIC, Jordi Girona 18-26, Barcelona 08034, Spain

^e Department of Medicine, Center for Biomedical Engineering, Brigham and Women's Hospital, Harvard Medical School, Cambridge, Massachusetts 02139, USA

^f Harvard–MIT Division of Health Sciences and Technology, Massachusetts Institute of Technology, Cambridge, Massachusetts 02139, USA

^g Wyss Institute for Biologically Inspired Engineering, Harvard University, Boston, Massachusetts 02115, USA

^h Department of Physics, King Abdulaziz University, Jeddah 21569, Saudi Arabia

ⁱ Department of Maxillofacial Biomedical Engineering and Institute of Oral Biology, School of Dentistry, Kyung Hee University, Seoul 130-701, Republic of Korea

† Electronic supplementary information (ESI) available. See DOI: 10.1039/c4lc00479e

hydrogel.¹² GelMA is a photopolymerizable, seminatural hydrogel composed of modified gelatin with methacrylic anhydride, and it is an attractive biomaterial for cell-based studies and tissue engineering applications.¹⁸ Dielectrophoretically manipulated cells can be preserved in their positions upon the crosslinking of the GelMA prepolymer induced by UV light. In this study, the latter approach was used to form 3D EBs within GelMA hydrogels.

There are several techniques available for forming EBs using the DEP approach. For example, Agarwal *et al.*¹⁹ used p-DEP to aggregate ESCs on microelectrodes. Different ESC aggregate sizes were formed as the electrode configuration was changed, and the cells survived for several days after applying DEP forces. However, the ESC aggregates were not in a spherical form. In another approach, Tsutsui *et al.*²⁰ used p-DEP to trap the ESCs in an array of poly(ethylene glycol) hydrogel microwells fabricated on a planar indium tin oxide (ITO) electrode. The captured cells subsequently formed viable and homogeneous monolayer patterns of ESCs. However, they did not exhibit a 3D spherical native EB structure. Spherical native-like EBs could not be obtained using these techniques because of the planar electrodes in the DEP devices. The EB formation took a considerably long time (*e.g.*, 24 h in Agarwal *et al.*'s work¹⁹). In addition, there was little control over the microenvironment of fabricated EBs. In contrast to previous studies, we report the formation of 3D spherical EBs with different sizes and shapes in photopolymerizable GelMA hydrogels in a rapid manner. Our DEP device was designed and fabricated in a 3D platform to obtain spatially homogeneous EB structures. Tuning the mechanical and biological characteristics of GelMA hydrogels is an efficient method to control stem cell fate and differentiation of cells cultured within them.

In this investigation, we report a novel method for rapidly forming 3D EBs in GelMA hydrogels using n-DEP in a high-throughput manner. The cells accumulated within 15 s at the intersections of electrode grids with relatively low electric fields enclosed with strong electric field regions (Fig. 1 and Movie S1†). The entire process took less than 6 min, which is a considerably short time to form stem cell aggregates and EBs compared with other conventional methods (*e.g.*, a few days using a hanging drop system⁵). The procedure of the present study was able to generate a vast number of EBs within a single device. Dielectrophoretically aggregated stem cells had 3D structures, as shown in Fig. 1F and Movie S2.†

Fig. S1† shows the calculated distribution of the applied electric field (voltage 12 V_{pp} and frequency 1.0 MHz) within the upper ITO-IDA and lower ITO-IDA electrodes. The phase applied to bands (a) and (i) was opposite to that applied to bands (b) and (ii). The simulation results show that cells prefer to accumulate within intersections (a-i) and (b-ii) as opposed to intersections (a-ii) and (b-i) because of the low electric fields in these regions. Furthermore, when the ratio of the electrode gap to the width is not identical, the 3D electric cell traps are not symmetrical and therefore the cells

adopt a 3D rhomboidal structure instead of a 3D spherical structure. The obtained simulation data were confirmed using 50 μm gap–50 μm width and 50 μm gap–150 μm width electrode devices (Fig. S1C†) as the cells formed 3D spherical and rhomboidal aggregates within these devices, respectively. Cell shape plays an important role in directing the fate of ESCs. McBeath *et al.*²¹ demonstrated that the stem cell shape regulates the commitment of mesenchymal stem cells (MSCs) to adipocyte or osteoblast lineages. Recently, Kilian *et al.*²² showed how the cell shape can be used to promote the differentiation of MSCs to distinct lineages. In our system, we can easily modify the electrode design to achieve different shapes of EBs.

EB size is another important parameter that affects stem cell fate and its early differentiation to different germ layers.²³ In our previous studies, we have demonstrated that the differentiation of ESCs can be regulated to a certain extent by controlling the size of the EBs.²⁴ In particular, when size-controlled cell aggregates were seeded on cell culture dishes, endothelialization was enhanced in smaller EBs (150 μm in diameter), while larger EBs (450 μm in diameter) differentiated towards cardiomyocytes. In the present study, we have demonstrated that it is feasible to control the size of stem cell aggregates by changing the electrode configuration. As can be seen in Fig. S2,† we obtained 3D cell aggregates with diameters ranging from 50 to 300 μm by increasing the distance between the band electrodes (Fig. S2B†). The total number of 3D cell aggregates that can be obtained on a device directly depends on the device size and the diameter of the aggregates. Here, the working area of the device was 0.9 cm × 0.9 cm. Therefore, 289 cell aggregates were obtained for the largest aggregate diameter ($\phi = 300 \mu\text{m}$) and 5400 cell aggregates were obtained for the smallest aggregate diameter ($\phi = 75 \mu\text{m}$) (Fig. S2D†). The structure of the 3D aggregates was spherical and independent of the size of the cell aggregates (Fig. S2C†). These data demonstrate that we have developed a system capable of controlling the size of EBs in a high-throughput manner.

3D spherical cell aggregates encapsulated in the GelMA hydrogel were cultivated in standard cell culture dishes for several days. The viability of the dielectrophoretically patterned cells was investigated using a live/dead assay at days 1 and 3 of culture. Fig. 2 presents stained pictures of 3D spherical cell aggregates of different diameters. Unpatterned stem cells were used as the control in the experiment. There was no statistically meaningful difference between the cell viability of the underlying samples at different culture times, and all samples showed high cellular viability (>90%). In addition, the expression level of the Nanog gene indicating the EB development was evaluated for the dielectrophoretically patterned and unpatterned cells after 1 week of cultivation. Nanog is a transcription factor in ESCs which regulates the pluripotency of stem cells. In non-differentiated stem cells, this factor is more up-regulated than in differentiated stem cells.²⁵ Here, the Nanog gene was significantly down-regulated for the 3D cell aggregates compared with that for

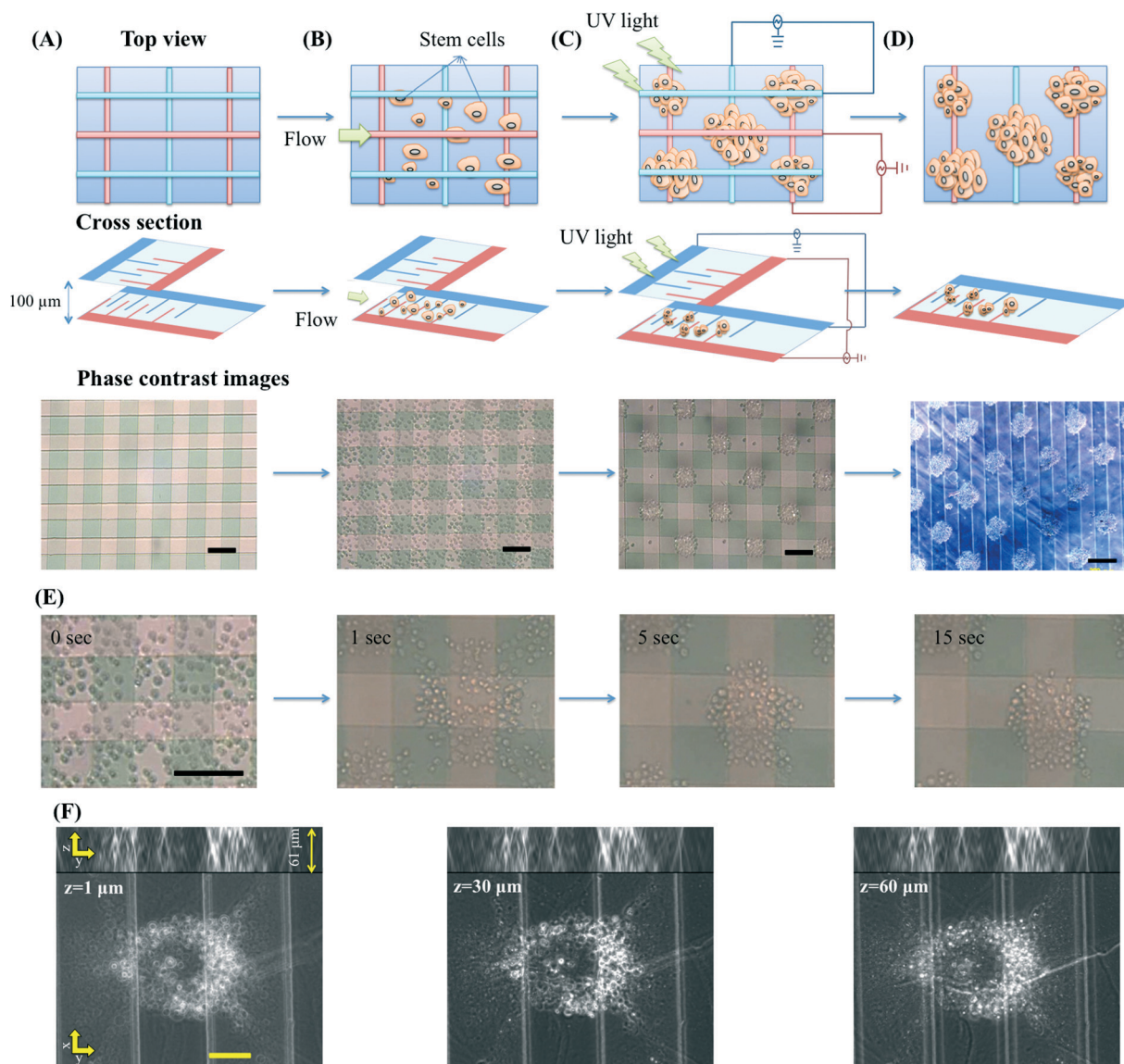


Fig. 1 Formation of 3D ESC aggregates in the GelMA hydrogel using DEP. (A) ITO-IDA electrodes were arranged face-to-face and a microfluidic chamber was maintained between them using a polyester film of 100 μm thickness. (B) The stem cells in the GelMA prepolymer were introduced into the 100 μm height chamber and (C) localized by n-DEP forces to the low electric field regions within the ITO-IDA electrodes. The GelMA prepolymer was then exposed to UV light, embedding the cells in a stable microscale organization. (D) Aggregated ESCs within the GelMA hydrogel were removed from the top IDA electrode and cultured. (E) Phase-contrast images of the ESC patterning over time. The ESCs were dielectrophoretically patterned within 15 s. (F) Phase-contrast images of ESC aggregates at different z-axis stacks indicating the 3D structure of stem cells. Projection of stem cells along the z- and y-axes is shown at the top of images. Scale bars: 50 μm.

the unpatterned cells (Fig. 2C). Note that after the formation of stem cell aggregates using the DEP method, they were cultured in an FBS-containing medium to induce differentiation. Dielectrophoretically fabricated EBs had higher pluripotency compared with single stem cells. Therefore, the differentiation of EBs was significantly higher than that of the single stem cells, leading to the lower expression of the *Nanog* gene in the EBs compared with that in the single stem cells after 7 days of culture in the differentiation medium. Taken together, successful 3D EB formation within the GelMA hydrogels (Fig. 2D and Movie S3†) and the ability of

the obtained EBs to differentiate to different cell types were demonstrated.

In conclusion, an ITO-IDA device was designed and fabricated to generate 3D stem cell aggregates using DEP. Dielectrophoretically assembled cells within GelMA hydrogels formed 3D spherical aggregates resembling the actual 3D structure of EBs. The 3D cell aggregates maintained their viability and started to differentiate upon culture. The proposed technique is efficient in manipulating stem cells into different shapes and sizes and is able to obtain a large number of EBs in a high-throughput manner.

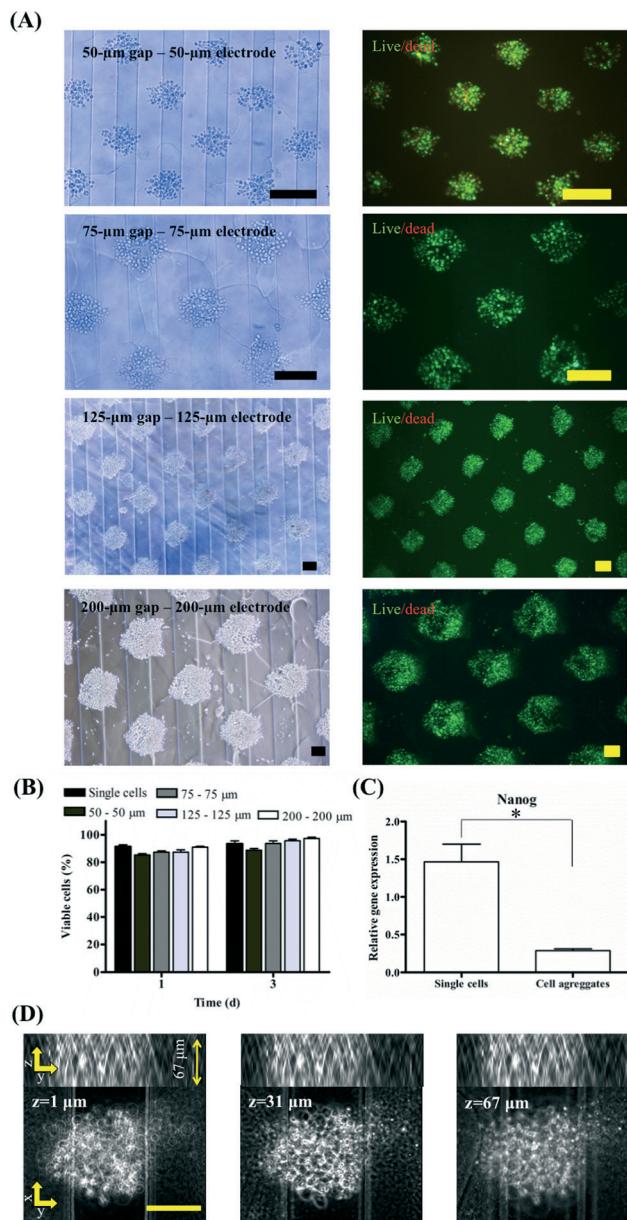


Fig. 2 Viability, differentiation, and structure of dielectrophoretically aggregated ESCs. (A) Optical and fluorescence images of live and dead cells as patterned by DEP and unpatterned cells at day 3 of culture. Scale bars: 100 μm. (B) Quantified results of the live/dead assay for the patterned and unpatterned ESCs. (C) Expression levels of Nanog for the dielectrophoretically patterned ESCs using a 125 μm gap–125 μm width electrode device and unpatterned ESCs at day 7 of culture. Expression levels were normalized with respect to the internal reference gene GAPDH (**p* < 0.05). (D) Phase-contrast images of EBs at different z-axis stacks, indicating the 3D structure of EBs at day 7 of culture. Projection of stem cells along the z- and y-axes is shown at the top of images. Scale bars: 50 μm.

Acknowledgements

S.A., S.Y., and J.R. designed the experiment and analyzed the results. S.Y. performed the experiments under the supervision of S.A. and J.R. J.R. wrote the paper. J.R., H.S., A.K., and T.M. supervised the whole project. All authors read the manuscript,

commented on it, and approved its content. This work was supported by the World Premier International Research Center Initiative (WPI), MEXT, Japan.

References

- 1 R. McKay, *Nature*, 2000, **406**, 361–364.
- 2 I. Desbaillets, U. Ziegler, P. Groscurth and M. Gassmann, *Exp. Physiol.*, 2000, **85**, 645–651.
- 3 M. A. Ramírez, E. Pericuesta, R. Fernández-González, B. Pintado and A. Gutiérrez-Adán, *Int. J. Dev. Biol.*, 2007, **51**, 397–408.
- 4 S. M. Dang, S. Gerecht-Nir, J. Chen, J. Itskovitz-Eldor and P. W. Zandstra, *Stem Cells*, 2004, **22**, 275–282.
- 5 S. M. Dang, M. Kyba, R. Perlingeiro, G. Q. Daley and P. W. Zandstra, *Biotechnol. Bioeng.*, 2002, **78**, 442–453.
- 6 A. Khademhosseini, J. Yeh, G. Eng, J. Karp, H. Kaji, J. Borenstein, O. C. Farokhzad and R. Langer, *Lab Chip*, 2005, **5**, 1380–1386.
- 7 M. Koike, S. Sakaki, Y. Amano and H. Kurosawa, *J. Biosci. Bioeng.*, 2007, **104**, 294–299.
- 8 S. Niebruegge, C. L. Bauwens, R. Peerani, N. Thavandiran, S. Masse, E. Sevaptisidis, K. Nanthakumar, K. Woodhouse, M. Husain, E. Kumacheva and P. W. Zandstra, *Biotechnol. Bioeng.*, 2009, **102**, 493–507.
- 9 S. Ostrovidov, V. Hosseini, S. Ahadian, T. Fujie, S. P. Parthiban, M. Ramalingam, H. Bae, H. Kaji and A. Khademhosseini, *Tissue Eng., Part B*, 2014, DOI: 10.1089/ten.teb.2013.0534.
- 10 R. Obregón, J. Ramón-Azcón, S. Ahadian, H. Shiku, H. Bae, M. Ramalingam and T. Matsue, *J. Nanosci. Nanotechnol.*, 2014, **14**, 487–500.
- 11 A. Khademhosseini, R. Langer, J. Borenstein and J. P. Vacanti, *Proc. Natl. Acad. Sci. U. S. A.*, 2006, **103**, 2480–2487.
- 12 J. Ramón-Azcón, S. Ahadian, R. Obregon, G. Camci-Unal, S. Ostrovidov, V. Hosseini, H. Kaji, K. Ino, H. Shiku, A. Khademhosseini and T. Matsue, *Lab Chip*, 2012, **12**, 2959–2969.
- 13 M. Yamamoto, T. Yasukawa, M. Suzuki, S. Kosuge, H. Shiku, T. Matsue and F. Mizutani, *Electrochim. Acta*, 2012, **82**, 35–42.
- 14 S. Ahadian, J. Ramón-Azcón, M. Estili, R. Obregón, H. Shiku and T. Matsue, *Biosens. Bioelectron.*, 2014, **59**, 166–173.
- 15 S. Ahadian, J. Ramón-Azcón, M. Estili, X. Liang, S. Ostrovidov, H. Shiku, M. Ramalingam, K. Nakajima, Y. Sakka, H. Bae, T. Matsue and A. Khademhosseini, *Sci. Rep.*, 2014, **4**, 4271.
- 16 R. Obregón, S. Ahadian, J. Ramón-Azcón, L. Y. Chen, T. Fujita, H. Shiku, M. W. Chen and T. Matsue, *Biosens. Bioelectron.*, 2013, **50**, 194–201.
- 17 J. Lu, C. A. Barrios, A. R. Dickson, J. L. Nourse, A. P. Lee and L. A. Flanagan, *Integr. Biol.*, 2012, **4**, 1223–1236.
- 18 J. W. Nichol, S. T. Koshy, H. Bae, C. M. Hwang, S. Yamanlar and A. Khademhosseini, *Biomaterials*, 2010, **31**, 5536–5544.
- 19 S. Agarwal, A. Sebastian, L. M. Forrester and G. H. Markx, *Biomicrofluidics*, 2012, **6**, 024101–024111.

- 20 H. Tsutsui, E. Yu, S. Marquina, B. Valamehr, I. Wong, H. Wu and C.-M. Ho, *Ann. Biomed. Eng.*, 2010, **38**, 3777–3788.
- 21 R. McBeath, D. M. Pirone, C. M. Nelson, K. Bhadriraju and C. S. Chen, *Dev. Cell*, 2004, **6**, 483–495.
- 22 K. A. Kilian, B. Bugarija, B. T. Lahn and M. Mrksich, *Proc. Natl. Acad. Sci. U. S. A.*, 2010, **107**, 4872–4877.
- 23 C. L. Bauwens, R. Peerani, S. Niebruegge, K. A. Woodhouse, E. Kumacheva, M. Husain and P. W. Zandstra, *Stem Cells*, 2008, **26**, 2300–2310.
- 24 Y.-S. Hwang, B. G. Chung, D. Ortmann, N. Hattori, H.-C. Moeller and A. Khademhosseini, *Proc. Natl. Acad. Sci. U. S. A.*, 2009, **106**, 16978–16983.
- 25 K. Okita, T. Ichisaka and S. Yamanaka, *Nature*, 2007, **448**, 313–317.